

# Quantum reactive scattering of ultracold $\text{NH}(X^3\Sigma^-)$ radicals in a magnetic trap

Liesbeth M. C. Janssen,\* Ad van der Avoird, and Gerrit C. Groenenboom†

*Radboud University Nijmegen, Institute for Molecules and Materials,*

*Heyendaalseweg 135, 6525 AJ Nijmegen, The Netherlands*

(Dated: May 13, 2018)

We investigate the ultracold reaction dynamics of magnetically trapped  $\text{NH}(X^3\Sigma^-)$  radicals using rigorous quantum scattering calculations involving three coupled potential energy surfaces. We find that the reactive  $\text{NH} + \text{NH}$  cross section is driven by a short-ranged collisional mechanism, and its magnitude is only weakly dependent on magnetic field strength. Unlike most ultracold reactions observed so far, the  $\text{NH} + \text{NH}$  scattering dynamics is non-universal. Our results indicate that chemical reactions can cause more trap loss than spin-inelastic  $\text{NH} + \text{NH}$  collisions, making molecular evaporative cooling more difficult than previously anticipated.

The ability to produce and trap molecules at sub-kelvin temperatures offers numerous exciting possibilities in chemistry. Recent experiments have demonstrated that ultracold chemical reactions can be efficiently manipulated using an external electromagnetic field [1–3], providing new tools to control reaction pathways and rate constants. The pronounced quantum behavior of ultracold matter may also lead to novel phenomena such as “superchemistry”, a process in which an atomic and molecular Bose-Einstein condensate (BEC) are coherently coupled to stimulate chemical reactivity [4]. Up to the present, however, studies on ultracold chemical reactions have focused only on (bi-)alkali-metal systems with a rather limited chemistry. Moreover, most of the observed ultracold reactive processes exhibit universal behavior, i.e., the dynamics are completely determined by long-range interactions [5]. Cold reactive collisions in the non-universal regime, as well as cold reactions involving non-alkali and open-shell molecules, are still largely unexplored.

Cold chemistry is also relevant in the context of evaporative and sympathetic cooling. These second-stage cooling methods, which rely on strong elastic collisions between trapped particles, represent the final step towards full quantum degeneracy and Bose-Einstein condensation [6]. As a rule of thumb, the ratio between elastic and non-elastic (inelastic and reactive) cross sections should be at least two orders of magnitude in order for second-stage cooling to succeed. For polar molecules, whose properties are expected to find wide applications in ultracold physics [7–11], cooling into the quantum-degenerate regime is yet to be achieved experimentally. Various theoretical studies suggest that molecular second-stage cooling is feasible [12–19], but these investigations are based on the assumption that chemical reactions are strongly suppressed in a (magnetically trapped) spin-polarized gas [20] and that the dynamics evolves on a single non-reactive potential. To our knowledge, this assumption has not yet been validated by explicit reactive scattering calculations.

In this Letter, we present rigorous coupled-channels calculations for the reactive  $\text{NH}(X^3\Sigma^-) + \text{NH}(X^3\Sigma^-)$  system in the presence of a magnetic field. Ultracold reactive  $\text{NH} + \text{NH}$  collisions can yield as many as eight different product arrangements [21, 22], making it a versatile system for cold chemistry studies.  $\text{NH}$  has already been cooled to millikelvin temperatures and stored in a magnetic trap using Stark decel-

eration [23, 24] and buffer gas cooling techniques [15, 25, 26], and earlier theoretical studies – based on non-reactive scattering calculations – have indicated that  $\text{NH}$  is a promising candidate for second-stage cooling experiments [12–17, 19, 27]. Within a magnetic trap,  $\text{NH}$  is polarized in the low-field-seeking state  $|S_{\text{NH}} = 1, M_{S_{\text{NH}}} = 1\rangle$ , with  $S_{\text{NH}}$  denoting the total electronic spin and  $M_{S_{\text{NH}}}$  its projection onto the magnetic field axis. A collision complex of two such molecules is in the high-spin quintet  $|S = 2, M_S = 2\rangle$  state, with  $S$  and  $M_S$  referring to the dimer spin quantum numbers. Spin-inelastic  $\text{NH} + \text{NH}$  collisions can change either the  $M_S$  quantum number of the quintet state or the total spin  $S$  to produce singlet ( $S = 0$ ) or triplet ( $S = 1$ ) complexes. Since the  $S = 0$  and 1 states are chemically reactive [21],  $S$ -changing transitions may also initiate chemical reaction.

In order to study the reaction dynamics of cold  $\text{NH}$  radicals, we have employed a single-arrangement quantum reactive scattering method that allows for the calculation of total  $\text{NH} + \text{NH}$  reaction probabilities. The cross sections are obtained from full quantum scattering calculations on three ( $S = 0, 1, 2$ ) coupled potential energy surfaces. Our results indicate that chemical reactions can cause more trap loss than inelastic collisions, implying that reactive channels must be taken into account when assessing the feasibility of evaporative and sympathetic cooling. We also find that the total reaction probability is strongly dependent on the details of the (short-range) interaction potentials, providing one of the first examples of non-universal cold chemistry.

We focus on collisions between two magnetically trapped bosonic  $^{15}\text{NH}(X^3\Sigma^-)$  molecules and treat the monomers as rigid rotors. The coordinate system consists of the intermolecular vector  $\mathbf{R}$ , with length  $R$ , the polar angles  $\theta_A$  and  $\theta_B$  of the monomers, and the dihedral angle  $\phi$ . The scattering Hamiltonian is given by

$$\begin{aligned} \hat{H} = & -\frac{\hbar^2}{2\mu R} \frac{\partial^2}{\partial R^2} R + \frac{\hat{L}^2}{2\mu R^2} \\ & + \sum_{S, M_S} |S, M_S\rangle V_S(R, \theta_A, \theta_B, \phi) \langle S, M_S| \\ & + V_{\text{magn.dip}}(\mathbf{R}, \hat{\mathbf{S}}_A, \hat{\mathbf{S}}_B) + \hat{H}_A + \hat{H}_B, \end{aligned} \quad (1)$$

where  $\mu$  is the reduced mass of the complex,  $\hat{L}^2$  is the angular momentum operator associated with rotation of  $\mathbf{R}$ ,

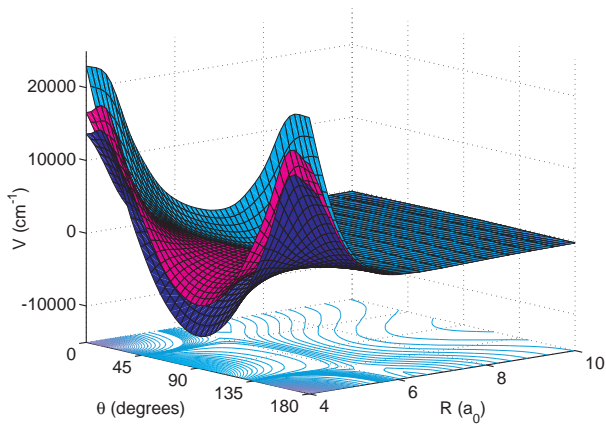


FIG. 1: Cuts through the quintet (cyan), triplet (magenta), and singlet (dark blue) potential energy surfaces of  $\text{NH}(X^3\Sigma^-) - \text{NH}(X^3\Sigma^-)$  for  $\phi = 180^\circ$  and  $\theta_A = \theta_B = \theta$ .

$V_S(R, \theta_A, \theta_B, \phi)$  is the potential energy surface for total spin  $S$ ,  $V_{\text{magn.dip}}(\mathbf{R}, \hat{\mathbf{S}}_A, \hat{\mathbf{S}}_B)$  is the intermolecular magnetic dipole interaction between the two monomer triplet spins, and  $\hat{H}_A$  and  $\hat{H}_B$  are the Hamiltonians of the individual monomers. The latter account for the monomer rotation, intramolecular spin-spin coupling, spin-rotation coupling, and Zeeman interaction [17]. The terms that couple the  $S = 0, 1$ , and  $2$  potentials and that ultimately drive spin-changing processes are the intermolecular magnetic dipole interaction and the intramolecular spin-spin and spin-rotation couplings.

The NH–NH potential energy surfaces have been obtained from high-level *ab initio* calculations, as described previously [28]. Figure 1 shows a cut through the three NH–NH potentials for  $\phi = 180^\circ$  and  $\theta_A = \theta_B = \theta$ . It can be seen that the singlet and triplet potentials are strongly attractive at small intermolecular distances, which is due to their chemically reactive nature. In view of these deep potential energy wells we may assume that, once a reactive singlet or triplet NH–NH complex is formed, the system readily undergoes exoergic chemical rearrangement. For instance,  $\text{NH} + \text{NH}$  may react into  $\text{N}_2\text{H}_2$  (provided that a third body can dissipate the excess kinetic energy) or into a binary product configuration such as  $\text{N}_2 + \text{H}_2$  [22]. In order to calculate the total reaction probability, we consider only the NH + NH reactant arrangement and apply “capture” boundary conditions at short range. That is, at a sufficiently small value of the radial coordinate  $R$ , we allow flux to disappear into reactive channels. Such an approach is commonly used in (reactive) scattering problems involving deep potential energy wells [29]. We note that not all collisions on the singlet and triplet potentials are reactive, since these surfaces are repulsive for certain geometries. Hence,  $S$ -changing collisions will not necessarily lead to chemical reaction. This is also contained in our boundary conditions (see Supplementary Material). Collisions occurring on the quintet potential are entirely non-reactive.

We have developed a novel reactive scattering algorithm based on the renormalized Numerov propagator to calculate

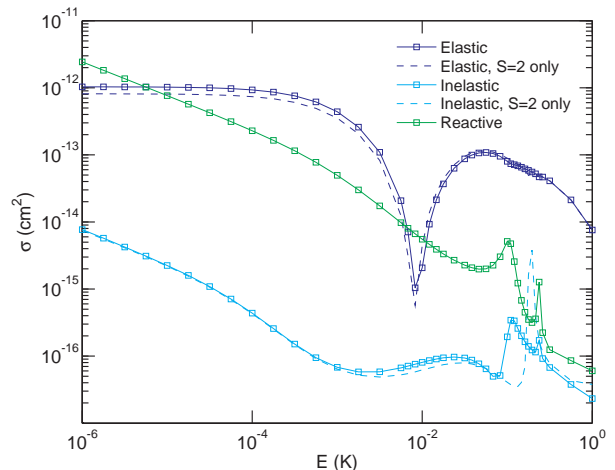


FIG. 2: Cross sections for magnetically trapped  $^{15}\text{NH} + ^{15}\text{NH}$  as a function of collision energy, calculated for a magnetic field strength of 1 G. The solid lines were obtained by including all three potentials in the scattering calculations, while the dashed lines were obtained using only the non-reactive quintet potential.

the relevant collision cross sections. Our algorithm amounts to solving the coupled-channels equations for *two* sets of solutions, and subsequently applying reactive scattering boundary conditions to obtain the  $S$ -matrix. Details can be found in the Supplementary Material. We used a symmetry-adapted channel basis set with even permutation symmetry and even parity, and a space-fixed total angular momentum projection of  $\mathcal{M} = 2$  (see also Supplementary Material). This basis allows for  $s$ -wave collisions between identical bosonic molecules in the same initial quantum state. The radial grid ranged from 4.5 to  $1500 a_0$ , with a minimum of 10 grid points per smallest (local) de Broglie wavelength. The cross sections were calculated for collision energies  $E$  of  $10^{-6}$  to 1 K and magnetic field strengths  $B$  of  $10^{-1}$  to  $10^4$  G.

Figure 2 shows the elastic, spin-inelastic, and reactive cross sections for two magnetically trapped NH molecules as a function of the collision energy for  $B = 1$  G. We find that the elastic cross section at small  $E$  is constant as a function of energy, consistent with Wigner’s threshold law for  $s$ -wave elastic scattering [30],  $\sigma_{\text{elastic}} \propto E^{L_{\text{in}} + L_{\text{out}}}$ . Here  $L_{\text{in}}$  and  $L_{\text{out}}$  denote the partial waves for the incoming and outgoing channels, respectively. The inelastic and reactive cross sections exhibit  $E^{-1/2}$  threshold behavior, as expected from the  $E^{L_{\text{in}} - 1/2}$  law for exoergic  $s$ -wave ( $L_{\text{in}} = 0$ ) collisions [30]. In order to compare our results with the non-reactive case, we have also plotted the cross sections obtained from scattering calculations on the non-reactive quintet potential. As can be seen in Fig. 2, the inclusion of chemically reactive ( $S = 0$  and  $1$ ) potentials has an almost negligible effect on the elastic and spin-inelastic cross sections, confirming our earlier expectations reported in Ref. [27]. We thus conclude that most of the non-reactive, inelastic trap loss occurs on the quintet surface, and that collisions on the  $S = 0$  and  $1$  potentials are almost 100% reactive.

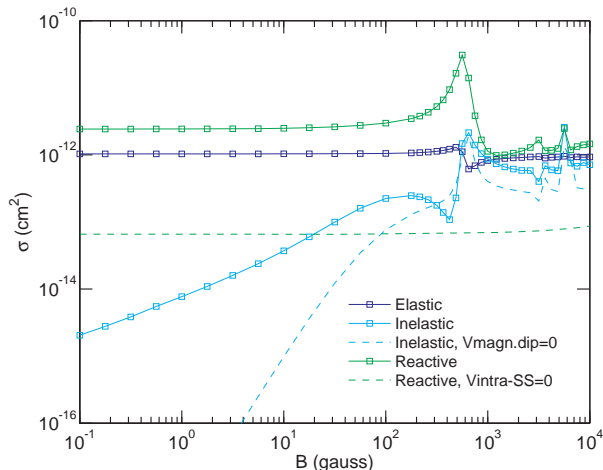


FIG. 3: Cross sections for magnetically trapped  $^{15}\text{NH} + ^{15}\text{NH}$  as a function of magnetic field strength, calculated at  $E = 10^{-6}$  K. The spin-inelastic cross sections obtained with the intermolecular magnetic dipole term switched off, and the reactive cross sections obtained with the intramolecular spin-spin coupling switched off, are also plotted.

Figure 2 also indicates that (for  $B = 1$  G) the elastic-to-reactive cross section ratio is much smaller than the elastic-to-inelastic ratio, the difference being 2 to 3 orders of magnitude. This leads us to reconsider the prospects for molecular evaporative cooling. While previous studies based on non-reactive scattering calculations have found that evaporative cooling of NH is feasible [17, 19, 27], our present results indicate that chemical reactions can pose a major constraint on the efficiency of the cooling process. Thus, second-stage cooling of NH might be more difficult than previously expected. We will return to this topic later, when discussing the effect of uncertainties in the potentials.

In Fig. 3, we present the collision cross sections as a function of magnetic field for a collision energy of  $10^{-6}$  K. We have already established in previous work [17, 31] that the intermolecular magnetic dipolar term is the dominant source of inelastic trap loss at ultralow energies. Indeed, when discarding the intermolecular magnetic dipole-dipole coupling ( $V_{\text{magn.dip}}$ ) in our reactive scattering calculations, the spin-inelastic cross section decreases by several orders of magnitude. For the *reactive* cross sections, however, we find that the main contribution comes from the *intramolecular* spin-spin coupling (denoted as  $V_{\text{intra-SS}}$  in Fig. 3). The effect of the intermolecular term  $V_{\text{magn.dip}}$  on the chemical reactivity is almost negligible. This can also be understood by considering that the intermolecular spin-spin interaction is long-ranged [31], while a chemical reaction can only proceed when the reactants approach each other to a very short distance. Hence, the intramolecular spin-spin coupling, which acts through the potential anisotropy at short range [32, 33], plays the most important role in enabling the reaction to occur.

It may also be seen that the reactive cross section at small fields ( $B < 100$  G) is constant as a function of  $B$ . This

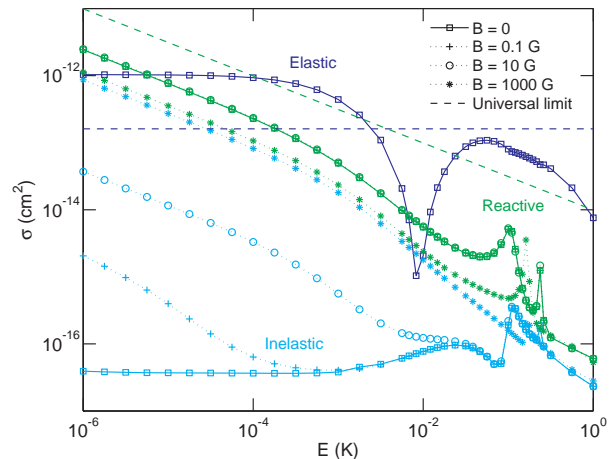


FIG. 4: Cross sections for magnetically trapped  $^{15}\text{NH} + ^{15}\text{NH}$  as a function of collision energy, calculated for several magnetic field strengths. The elastic cross sections are the same for all magnetic fields considered, and the reactive cross sections are the same for  $B = 0, 0.1,$  and  $10$  G. The results of the universal quantum-defect model are also shown.

is essentially a consequence of the  $E^{L_{\text{in}}-1/2}$  law for exoergic collisions: the threshold behavior is determined only by the centrifugal barrier in the entrance channel, and the energy of the outgoing (reactive) channel has no effect on the cross section. Note that a different threshold law applies for short-range-induced *inelastic* processes, for which the centrifugal barrier and energy of the outgoing channel do play a role [34].

Figure 4 compares the scattering results for different magnetic field strengths, including  $B = 0$ , as a function of collision energy. We find that the reactive cross sections are independent of magnetic field for  $B < 100$  G at virtually all energies considered, and the  $\{B^0, E^{L_{\text{in}}-1/2}\}$  regime extends down to  $B = 0$ . The *inelastic* cross sections, however, are different for all  $B$  values, and they become constant as a function of energy for  $B = 0$  [36]. Thus, the reactive and inelastic cross sections show fundamentally different behavior in the ultracold regime.

Let us now consider ultracold NH + NH scattering in the universal limit. Knowledge of the degree of universality is useful to understand and interpret the (generally complex) full-dimensional reaction dynamics in terms of simple few-parameter models. In order to establish whether the ultracold chemistry of NH + NH is universal, we compare our scattering results with the single-channel quantum-defect model of Idziaszek and Julienne [5]. Details of this model are given in the Supplementary Material. In the universal limit, all scattering flux that reaches the short range disappears into reactive channels. Figure 4 compares the results of the universal quantum-defect model with those of the numerical coupled-channels calculations. In the *s*-wave regime ( $E < 10^{-3}$  K), the elastic cross sections are underestimated by the universal model, while the reactive cross sections are clearly overestimated. The *ratio* between the universal elastic and reactive

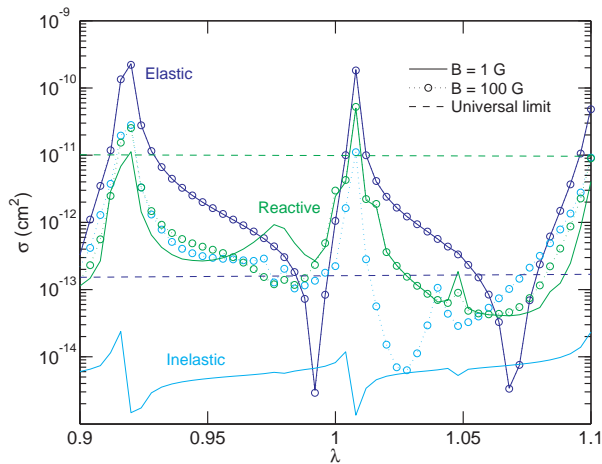


FIG. 5: Cross sections for magnetically trapped  $^{15}\text{NH} + ^{15}\text{NH}$  as a function of the scaling factor  $\lambda$ , calculated for two magnetic field strengths ( $B = 1$  and  $100$  G) at  $E = 10^{-6}$  K. The results of the universal quantum-defect model are also shown.

cross sections differs by more than one order of magnitude (a factor of  $\approx 26$ ) from the numerical data. These differences suggest that the  $\text{NH} + \text{NH}$  reaction dynamics is non-universal, because a significant fraction of the incident flux is reflected at short range. It should be noted, however, that the quantum-defect results apply to single-channel scattering on a single isotropic potential, while the numerical data have been obtained from multi-channel calculations on three coupled anisotropic potential energy surfaces. Nevertheless, the collision dynamics in the ultracold regime is  $s$ -wave dominated, and the effective  $\text{NH}$ – $\text{NH}$  long-range potential – which is the same for all three spin states – is governed mainly by the isotropic interaction. Thus, the single-channel quantum-defect model should be applicable to  $\text{NH}$ – $\text{NH}$  in the universal regime.

An alternative way to establish the degree of universality is to test the effect of small modifications in the (short-range) potentials. If the scattering is universal, the cross sections are completely determined by the long-range features of the interaction potentials. For instance, a scaling of the potentials by a factor of  $\lambda$  (or, equivalently, a scaling of the reduced mass by  $\lambda$ ) should change the universal elastic cross section by  $\lambda^{1/2}$ . Figure 5 shows the universal quantum-defect results as a function of the scaling parameter  $\lambda$  ( $0.9 \leq \lambda \leq 1.1$ ) for  $E = 10^{-6}$  K. The corresponding numerical cross sections, obtained by reduced-mass scaling, are also shown for  $B = 1$  and  $100$  G. It is evident that the numerical results are highly sensitive to the details of the potentials, and that the universal model is inaccurate for all values of  $\lambda$ . In fact, the resonance features in the numerical cross sections are signatures of non-universal behavior [35] and highlight the importance of short-range physics in the dynamics. We thus conclude that the scattering properties of magnetically trapped  $\text{NH}$  cannot be captured in a universal model.

As discussed extensively in Refs. [16, 17, 27], the  $\lambda$ -scaling

approach also provides a means to sample the effects of uncertainties in the interaction potentials. Although the potentials have been obtained from state-of-the-art methods, there is a small remaining inaccuracy in the *ab initio* data which gives rise to an uncertainty in the calculated cross sections. This also carries implications for the prospects for molecular evaporative cooling. More specifically, one should evaluate the elastic-to-reactive cross section ratio for all relevant  $\lambda$  values to obtain a realistic estimate of the cooling efficiency. In the case of  $\lambda = 1$ , we find that reactive  $\text{NH} + \text{NH}$  collisions are more probable than elastic ones (cf. Figs. 3 and 4), while for  $\lambda \approx 0.95$  and  $\lambda \approx 1.03$  the elastic cross sections are about one order of magnitude larger than the reactive ones. These results suggest that evaporative cooling of magnetically trapped  $\text{NH}$  might still be feasible, but the probability of success is significantly smaller than estimated earlier from non-reactive scattering calculations. We note that these findings are still valid when the size of the channel basis set is increased, as detailed in the Supplementary Material.

It can also be seen in Fig. 5 that the inelastic cross sections change rather dramatically from  $B = 1$  to  $100$  G, while the reactive cross sections show only a weak dependence on magnetic field. Nevertheless, for certain values of  $\lambda$ , the reactivity can increase by almost one order of magnitude as the magnetic field strength is changed. Thus, it may be possible to control the  $\text{NH} + \text{NH}$  reaction rate by means of an external field. For most  $\lambda$  values, however, the reactive cross sections show  $B^0$  behavior and magnetic field control will not be possible. We note that the final product-state distribution might be more sensitive to the magnetic field strength than the *total* reaction probability, but our scattering method does not allow the calculation of product-state-resolved reaction cross sections.

In summary, we have presented the first rigorous quantum scattering study of ultracold reactive molecular collisions in the presence of a magnetic field. Our results illustrate the importance of chemical reactions in a magnetically trapped molecular gas, and call to reconsider the prospects for molecular evaporative cooling and magnetically-controlled cold chemistry. This work may serve as a benchmark for other ultracold paramagnetic and dipolar molecules, the dynamics of which are still virtually unexplored.

LMCJ and GCG thank the Council for Chemical Sciences of the Netherlands Organization for Scientific Research (CW-NWO) for financial support. AvdA thanks the Alexander von Humboldt Foundation for a Humboldt Research Award.

\* Electronic mail: ljanssen@science.ru.nl

† Electronic mail: gerritg@theochem.ru.nl

- [1] K.-K. Ni, S. Ospelkaus, D. Wang, G. Quémener, B. Neyenhuis, M. H. G. de Miranda, J. L. Bohn, J. Ye, and D. S. Jin, *Nature* **464**, 1324 (2010).
- [2] S. Knoop, F. Ferlaino, M. Berninger, M. Mark, H.-C. Nägerl, R. Grimm, J. P. D’Incao, and B. D. Esry, *Phys. Rev. Lett.* **104**,

- 053201 (2010).
- [3] M. H. G. de Miranda, A. Chotia, B. Neyenhuis, D. Wang, G. Quémener, S. Ospelkaus, J. L. Bohn, J. Ye, and D. S. Jin, *Nat. Phys.* **7**, 502 (2011).
- [4] D. J. Heinzen, R. Wynar, P. D. Drummond, and K. Kheruntsyan, *Phys. Rev. Lett.* **84**, 5029 (2000).
- [5] Z. Idziaszek and P. S. Julienne, *Phys. Rev. Lett.* **104**, 113202 (2010).
- [6] W. Ketterle and N. J. van Druten, *Adv. Atom. Mol. Opt. Phys.* **37**, 181 (1996).
- [7] D. DeMille, *Phys. Rev. Lett.* **88**, 067901 (2002).  
D. DeMille, *Phys. Rev. Lett.* **88**, 067901 (2002).
- [8] A. Micheli, G. K. Brennen, and P. Zoller, *Nat. Phys.* **2**, 341 (2006).
- [9] T. Zelevinsky, S. Kotochigova, and J. Ye, *Phys. Rev. Lett.* **100**, 043201 (2008).
- [10] L. D. Carr, D. DeMille, R. V. Krems, and J. Ye, *New J. Phys.* **11**, 055049 (2009).
- [11] C. Chin, V. V. Flambaum, and M. G. Kozlov, *New J. Phys.* **11**, 055048 (2009).
- [12] A. O. G. Wallis and J. M. Hutson, *Phys. Rev. Lett.* **103**, 183201 (2009).
- [13] M. L. González-Martínez and J. M. Hutson, *Phys. Rev. A* **84**, 052706 (2011).
- [14] A. O. G. Wallis, E. J. J. Longdon, P. S. Żuchowski, and J. M. Hutson, *Eur. Phys. J. D* (2011).
- [15] M. T. Hummon, T. V. Tscherbul, J. Kłos, H.-I. Lu, E. Tsikata, W. C. Campbell, A. Dalgarno, and J. M. Doyle, *Phys. Rev. Lett.* **106**, 053201 (2011).
- [16] P. S. Żuchowski and J. M. Hutson, *Phys. Chem. Chem. Phys.* **13**, 3669 (2011).
- [17] L. M. C. Janssen, P. S. Żuchowski, A. van der Avoird, G. C. Groenenboom, and J. M. Hutson, *Phys. Rev. A* **83**, 022713 (2011).
- [18] T. V. Tscherbul, H.-G. Yu, and A. Dalgarno, *Phys. Rev. Lett.* **106**, 073201 (2011).
- [19] Y. V. Suleimanov, T. V. Tscherbul, and R. V. Krems, *J. Chem. Phys.* **137**, 024103 (2012).
- [20] R. V. Krems, *Phys. Chem. Chem. Phys.* **10**, 4079 (2008).
- [21] C.-H. Lai, M.-D. Su, and S.-Y. Chu, *J. Phys. Chem. A* **107**, 2700 (2003).
- [22] L. A. Poveda, M. Biczysko, and A. J. C. Varandas, *J. Chem. Phys.* **131**, 044309 (2009).
- [23] S. Hoekstra, M. Metsälä, P. C. Zieger, L. Scharfenberg, J. J. Gilijamse, G. Meijer, and S. Y. T. van de Meerakker, *Phys. Rev. A* **76**, 063408 (2007).
- [24] J. Riedel, S. Hoekstra, W. Jäger, J. J. Gilijamse, S. Y. T. van de Meerakker, and G. Meijer, *Eur. Phys. J. D* **65**, 161 (2011).
- [25] W. C. Campbell, E. Tsikata, H.-I. Lu, L. D. van Buuren, and J. M. Doyle, *Phys. Rev. Lett.* **98**, 213001 (2007).
- [26] M. T. Hummon, W. C. Campbell, H.-I. Lu, E. Tsikata, Y. Wang, and J. M. Doyle, *Phys. Rev. A* **78**, 050702 (2008).
- [27] L. M. C. Janssen, P. S. Żuchowski, A. van der Avoird, J. M. Hutson, and G. C. Groenenboom, *J. Chem. Phys.* **134**, 124309 (2011).
- [28] L. M. C. Janssen, G. C. Groenenboom, A. van der Avoird, P. S. Żuchowski, and R. Podeszwa, *J. Chem. Phys.* **131**, 224314 (2009).
- [29] S. J. Klippenstein and Y. Georgievskii, in *Low Temperatures And Cold Molecules*, edited by I. W. M. Smith, (World Scientific, London, 2008), pp. 175–229.
- [30] E. P. Wigner, *Phys. Rev.* **73**, 1002 (1948).
- [31] L. M. C. Janssen, A. van der Avoird, and G. C. Groenenboom, *Eur. Phys. J. D* **65**, 177 (2011).
- [32] R. V. Krems and A. Dalgarno, *J. Chem. Phys.* **120**, 2296 (2004).
- [33] R. V. Krems, H. R. Sadeghpour, A. Dalgarno, D. Zgid, J. Kłos, and G. Chałasiński, *Phys. Rev. A* **68**, 051401 (2003).
- [34] A. Volpi and J. L. Bohn, *Phys. Rev. A* **65**, 052712 (2002).
- [35] Z. Idziaszek, G. Quémener, J. L. Bohn, and P. S. Julienne, *Phys. Rev. A* **82**, 020703 (2010).
- [36] The threshold behavior for the  $V_{\text{magn.dip}}$ -induced inelastic cross section in a nonzero magnetic field has already been discussed in Ref. [31]. There it was shown that the cross section for  $B > 0$  shows an  $E^0$  regime for moderately low collision energies, and an  $E^{-1/2}$  regime for ultralow energies. As the magnetic field decreases, the  $E^0$  regime extends to an increasingly large range of  $E$ . Using a similar approach based on the Born approximation, it can be shown that the inelastic cross section in *zero* field is constant for *all* energies below some critical  $E$ . That is, the  $E^0$  regime extends to  $E = 0$  for  $B = 0$  (to be published).